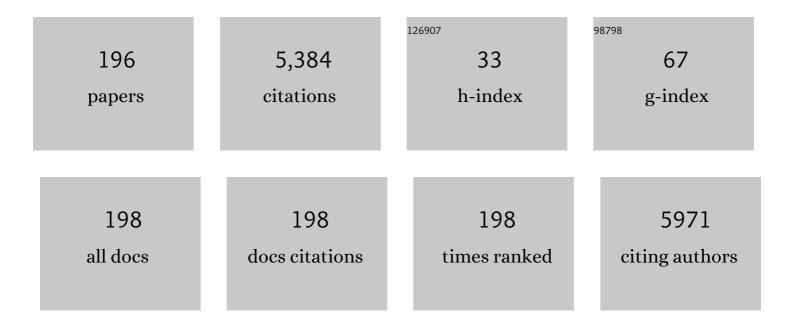
Tomoyuki Koganezawa

List of Publications by Year in descending order

Source: https://exaly.com/author-pdf/6846584/publications.pdf

Version: 2024-02-01



#	Article	IF	CITATIONS
1	Naphthobispyrazine Bisimide: A Strong Acceptor Unit for Conjugated Polymers Enabling Highly Coplanar Backbone, Short π–π Stacking, and High Electron Transport. Chemistry of Materials, 2022, 34, 2717-2729.	6.7	15
2	Synthesis of a novel A-b-(B-co-C)-type terpolymer with a regioregular poly(3-hexylthiophene) segment and its application to intrinsically stretchable transistor memory. Materials Chemistry and Physics, 2022, 281, 125911.	4.0	2
3	Exploring Charge Transport in Highâ€Temperature Polymorphism of ITIC Derivatives in Simple Processed Unipolar Bottom Contact Organic Fieldâ€Effect Transistor. Advanced Electronic Materials, 2022, 8, .	5.1	7
4	In situ high-temperature X-ray diffraction measurements of Pb(Zr _{0.58} Ti _{0.42})O ₃ epitaxial thin films grown on Si substrates. Japanese Journal of Applied Physics, 2022, 61, SN1012.	1.5	4
5	Exploration of Alkyl Group Effects on the Molecular Packing of 5,15-Disubstituted Tetrabenzoporphyrins toward Efficient Charge-Carrier Transport. ACS Applied Materials & Interfaces, 2022, 14, 32319-32329.	8.0	4
6	Improved ultraviolet stability of fullerene-based organic solar cells through light-induced enlargement and crystallization of fullerene domains. Thin Solid Films, 2022, 757, 139394.	1.8	1
7	Thickness dependencies of SiO2/BaOx layers on interfacial properties of a layered gate dielectric on 4H-SiC. Materials Science in Semiconductor Processing, 2021, 121, 105343.	4.0	1
8	Comparative Study of Selenophene- and Thiophene-Containing n-Type Semiconducting Polymers for High Performance All-Polymer Solar Cells. ACS Applied Polymer Materials, 2021, 3, 49-59.	4.4	9
9	Prolongation of the singlet exciton lifetime of nonfullerene acceptor films by the replacement of the central benzene core with naphthalene. Sustainable Energy and Fuels, 2021, 5, 2028-2035.	4.9	5
10	Monitoring of Crystallization Process in Solution-Processed Pentacene Thin Films by Chemical Conversion Reactions. Journal of Physical Chemistry C, 2021, 125, 2437-2445.	3.1	2
11	Interface Structures and Electronic States of Epitaxial Tetraazanaphthacene on Single-Crystal Pentacene. Materials, 2021, 14, 1088.	2.9	7
12	Analytical System for Simultaneous Operando Measurements of Electrochemical Reaction Rate and Hard X-ray Photoemission Spectroscopy. Journal of the Electrochemical Society, 2021, 168, 054506.	2.9	1
13	Insights into Microscopic Crystal Growth Dynamics of CH ₃ NH ₃ PbI ₃ under a Laser Deposition Process Revealed by <i>In Situ</i> X-ray Diffraction. ACS Applied Materials & Interfaces, 2021, 13, 22559-22566.	8.0	3
14	Molecular arrangement in diphenylanthracene derivative films deposited under vacuum on in-plane oriented polythiophene films. Japanese Journal of Applied Physics, 2021, 60, 085504.	1.5	1
15	Substrate-Independent Control of Polymorphs in Tetraphenylporphyrin Thin Films by Varying the Solvent Evaporation Time Using a Simple Spin-Coating Technique. Crystal Growth and Design, 2021, 21, 5116-5125.	3.0	4
16	Epitaxial pillar–matrix nanocomposite thin films of Bi–Ti–Fe–O and CoFe2O4 grown on SrTiO3 (110). Journal of Applied Physics, 2021, 130, 084101.	2.5	1
17	A comparative study of honeycomb-like 2D π-conjugated metal–organic framework chemiresistors: conductivity and channels. Dalton Transactions, 2021, 50, 13236-13245.	3.3	17
18	Extended π-Electron Delocalization in Quinoid-Based Conjugated Polymers Boosts Intrachain Charge Carrier Transport. Chemistry of Materials, 2021, 33, 8183-8193.	6.7	17

#	Article	IF	CITATIONS
19	Effect of Terminal-Group Halogenation of Naphthalene-Based Nonfullerene Acceptors on Their Film Structure and Photophysical and Photovoltaic Properties. ACS Applied Energy Materials, 2021, 4, 14022-14033.	5.1	5
20	Quasi-Homoepitaxial Junction of Organic Semiconductors: A Structurally Seamless but Electronically Abrupt Interface between Rubrene and Bis(trifluoromethyl)dimethylrubrene. Journal of Physical Chemistry Letters, 2021, 12, 11430-11437.	4.6	7
21	Impact of Noncovalent Sulfur–Fluorine Interaction Position on Properties, Structures, and Photovoltaic Performance in Naphthobisthiadiazoleâ€Based Semiconducting Polymers. Advanced Energy Materials, 2020, 10, 1903278.	19.5	39
22	Substrate-driven switchable molecular orientation in bulk heterojunction films identified using infrared reflection absorption spectroscopy. Molecular Systems Design and Engineering, 2020, 5, 559-564.	3.4	5
23	Orbital-Energy Modulation of Tetrabenzoporphyrin-Derived Non-Fullerene Acceptors for Improved Open-Circuit Voltage in Organic Solar Cells. Journal of Organic Chemistry, 2020, 85, 168-178.	3.2	10
24	Designing High Performance Nonfullerene Electron Acceptors with Rylene Imides for Efficient Organic Photovoltaics. Chemistry of Materials, 2020, 32, 195-204.	6.7	32
25	Elucidating the impact of molecular weight on morphology, charge transport, photophysics and performance of all-polymer solar cells. Journal of Materials Chemistry A, 2020, 8, 21070-21083.	10.3	23
26	Epitaxial L1-FeNi films with high degree of order and large uniaxial magnetic anisotropy fabricated by denitriding FeNiN films. Applied Physics Letters, 2020, 116, .	3.3	13
27	Efficient Exciton Diffusion in Micrometer-Sized Domains of Nanographene-Based Nonfullerene Acceptors with Long Exciton Lifetimes in Blend Films with Conjugated Polymer. ACS Applied Materials & Interfaces, 2020, 12, 39236-39244.	8.0	10
28	Layer-by-Layer Growth Control of Metal–Organic Framework Thin Films Assembled on Polymer Films. ACS Applied Materials & Interfaces, 2020, 12, 50784-50792.	8.0	22
29	Electronic and Crystallographic Examinations of the Homoepitaxially Grown Rubrene Single Crystals. Materials, 2020, 13, 1978.	2.9	9
30	Direct Correlation of Nanoscale Morphology and Device Performance to Study Photocurrent Generation in Donor-Enriched Phases of Polymer Solar Cells. ACS Applied Materials & Interfaces, 2020, 12, 28404-28415.	8.0	7
31	Solution-Processable Organic Semiconductors Featuring S-Shaped Dinaphthothienothiophene (S-DNTT): Effects of Alkyl Chain Length on Self-Organization and Carrier Transport Properties. Chemistry of Materials, 2020, 32, 5350-5360.	6.7	33
32	High-Throughput and Autonomous Grazing Incidence X-ray Diffraction Mapping of Organic Combinatorial Thin-Film Library Driven by Machine Learning. ACS Combinatorial Science, 2020, 22, 348-355.	3.8	9
33	Effects of a Fluorinated Donor Polymer on the Morphology, Photophysics, and Performance of All-Polymer Solar Cells Based on Naphthalene Diimide–Arylene Copolymer Acceptors. ACS Applied Materials & Interfaces, 2020, 12, 16490-16502.	8.0	17
34	Efficient light-harvesting, energy migration, and charge transfer by nanographene-based nonfullerene small-molecule acceptors exhibiting unusually long excited-state lifetime in the film state. Chemical Science, 2020, 11, 3250-3257.	7.4	35
35	Structural investigation of ferroelectric BiFeO3–BaTiO3 solid solutions near the rhombohedral–pseudocubic phase boundary. Applied Physics Letters, 2020, 116, .	3.3	5
36	Epitaxial growth of CH3NH3PbI3 on rubrene single crystal. APL Materials, 2020, 8, .	5.1	11

#	Article	IF	CITATIONS
37	CF4:O2 surface etching for the improvement of contact resistance and high-temperature reliability in Ni/Nb ohmic contacts on n-type 4H-SiC. Japanese Journal of Applied Physics, 2020, 59, 056501.	1.5	2
38	Characterization of selectively oriented polycrystalline silicon thin films formed by multiline beam continuous-wave laser lateral crystallization with overlapping. Japanese Journal of Applied Physics, 2020, 59, 115504.	1.5	2
39	Selective growth of <i>α</i> -Fe ₂ O ₃ , <i>γ</i> -Fe ₂ O ₃ Fe ₃ O ₄ at low temperatures and under ambient pressure. Japanese Journal of Applied Physics, 2019, 58, 095504.	1.5	11
40	Performance of Si/PEDOT:PSS Solar Cell Controlled by Dipole Moment of Additives. Journal of Physical Chemistry C, 2019, 123, 20130-20135.	3.1	20
41	In situ residual stress analysis in a phenolic resin and copper composite material during curing. Polymer, 2019, 182, 121857.	3.8	14
42	Synthesis and Deformable Hierarchical Nanostructure of Intrinsically Stretchable ABA Triblock Copolymer Composed of Poly(3-hexylthiophene) and Polyisobutylene Segments. ACS Applied Polymer Materials, 2019, 1, 315-320.	4.4	29
43	Alternative Face-on Thin Film Structure of Pentacene. Scientific Reports, 2019, 9, 579.	3.3	40
44	Evolution of crystallinity at a well-defined molecular interface of epitaxial C ₆₀ on the single crystal rubrene. Journal of Physics Condensed Matter, 2019, 31, 154001.	1.8	7
45	Fabrication of ionic liquid polycrystalline nano thin films and their ion conducting properties accompanied by solid-liquid phase transition. Thin Solid Films, 2019, 677, 77-82.	1.8	6
46	Fabrication of L10-type FeCo ordered structure using a periodic Ni buffer layer. AIP Advances, 2019, 9, 045307.	1.3	6
47	Understanding Comparable Charge Transport Between Edge-on and Face-on Polymers in a Thiazolothiazole Polymer System. ACS Applied Polymer Materials, 2019, 1, 1257-1262.	4.4	18
48	Molecular Orientation: Control of Molecular Orientation in Organic Semiconductor Films using Weak Hydrogen Bonds (Adv. Mater. 18/2019). Advanced Materials, 2019, 31, 1970131.	21.0	0
49	Control of Molecular Orientation in Organic Semiconductor Films using Weak Hydrogen Bonds. Advanced Materials, 2019, 31, e1808300.	21.0	62
50	New Random Copolymer Acceptors Enable Additive-Free Processing of 10.1% Efficient All-Polymer Solar Cells with Near-Unity Internal Quantum Efficiency. ACS Energy Letters, 2019, 4, 1162-1170.	17.4	134
51	Fabrication of <i>L</i> 1-FeNi by pulsed-laser deposition. Applied Physics Letters, 2019, 114, .	3.3	16
52	Widely Dispersed Intermolecular Valence Bands of Epitaxially Grown Perfluoropentacene on Pentacene Single Crystals. Journal of Physical Chemistry Letters, 2019, 10, 1312-1318.	4.6	17
53	Influence of Ni and Nb thickness on low specific contact resistance and high-temperature reliability of ohmic contacts to 4H-SiC. Japanese Journal of Applied Physics, 2019, 58, 116501.	1.5	5
54	Morphological Study of Blend Thin Films of Poly(3-hexylthiophene)- <i>block</i> -polyisobutylene- <i>block</i> -poly(3-hexylthiophene):F and Their Application to Photovoltaics, lowered of Photopolymor Science and Tochpology –	Poly(3-hexy	lthiophene)

and Their Application to Photovoltaics. Journal of Photopolymer Science and Technology = [Fotoporima Konwakai Shi], 2019, 32, 741-746.

#	Article	IF	CITATIONS
55	High-temperature reliability of Ni/Nb ohmic contacts on 4H-SiC for harsh environment applications. Thin Solid Films, 2019, 669, 306-314.	1.8	7
56	In Situ Residual Stress Analysis in a Glass-Fiber-Reinforced PhenolicResin and Copper Composite Material During Curing. Journal of the Adhesion Society of Japan, 2019, 55, 421-426.	0.0	1
57	Oriented thin films of mixture of a low-bandgap polymer and a fullerene derivative prepared by friction-transfer method. Japanese Journal of Applied Physics, 2018, 57, 02CA06.	1.5	2
58	Temperature Dependent Epitaxial Growth of C ₆₀ Overlayers on Single Crystal Pentacene. Advanced Materials Interfaces, 2018, 5, 1800084.	3.7	15
59	Fabrication of L10-FeNi phase by sputtering with rapid thermal annealing. Journal of Alloys and Compounds, 2018, 750, 164-170.	5.5	15
60	Surface crystallographic structures of cellulose nanofiber films and overlayers of pentacene. Japanese Journal of Applied Physics, 2018, 57, 03EE02.	1.5	3
61	Crystallization and Polymorphism of Organic Semiconductor in Thin Film Induced by Surface Segregated Monolayers. Scientific Reports, 2018, 8, 481.	3.3	21
62	Semiconducting silicon-tin alloy nanocrystals with direct bandgap behavior for photovoltaic devices. Materials Today Energy, 2018, 7, 87-97.	4.7	15
63	Conjugated Polyelectrolyte Blend with Polyethyleneimine Ethoxylated for Thickness-Insensitive Electron Injection Layers in Organic Light-Emitting Devices. ACS Applied Materials & Interfaces, 2018, 10, 17318-17326.	8.0	27
64	Formation of (100)-oriented large polycrystalline silicon thin films with multiline beam continuous-wave laser lateral crystallization. Japanese Journal of Applied Physics, 2018, 57, 031302.	1.5	13
65	Surface morphology of vacuum-evaporated pentacene film on Si substrate studied by in situ grazing-incidence small-angle X-ray scattering: I. The initial stage of formation of pentacene film. Japanese Journal of Applied Physics, 2018, 57, 03EG12.	1.5	1
66	In situ characterization of the film coverage and the charge transport in the alkylated-organic thin film transistor. Japanese Journal of Applied Physics, 2018, 57, 03EG14.	1.5	2
67	Improvement in interlayer structure of p–i–n-type organic solar cells with the use of fullerene-linked tetrabenzoporphyrin as additive. RSC Advances, 2018, 8, 35237-35245.	3.6	2
68	Effects of solvent vapor annealing on organic photovoltaics with a new type of solution-processable oligothiophene-based electronic donor material. Japanese Journal of Applied Physics, 2018, 57, 08RE09.	1.5	5
69	Growth-temperature-dependent coalescence determines structural phase of mist-chemical-vapor-deposition-grown SnO2 thin films. Journal of Applied Physics, 2018, 124, 125303.	2.5	6
70	Correlation between Distribution of Polymer Orientation and Cell Structure in Organic Photovoltaics. ACS Applied Materials & Interfaces, 2018, 10, 32420-32425.	8.0	16
71	Molecular orientation control of semiconducting molecules using a metal layer formed by wet processing. Organic Electronics, 2018, 63, 47-51.	2.6	11
72	Ionic Conductivity in Ionic Liquid Nano Thin Films. ACS Nano, 2018, 12, 10509-10517.	14.6	31

Τομογικι Koganezawa

#	Article	IF	CITATIONS
73	Structure control of a zinc tetraphenylporphyrin thin film by vapor annealing using fluorine containing solvent. Thin Solid Films, 2018, 665, 85-90.	1.8	5
74	Impact of the molecular quadrupole moment on ionization energy and electron affinity of organic thin films: Experimental determination of electrostatic potential and electronic polarization energies. Physical Review B, 2018, 97, .	3.2	47
75	All-Polymer Solar Cells with 9.4% Efficiency from Naphthalene Diimide-Biselenophene Copolymer Acceptor. Chemistry of Materials, 2018, 30, 6540-6548.	6.7	88
76	Organic Photovoltaic Devices Based on Oriented <i>n</i> -Type Molecular Films Deposited on Oriented Polythiophene Films. Journal of Nanoscience and Nanotechnology, 2018, 18, 2702-2710.	0.9	4
77	Organic Solar Cells with Controlled Nanostructures Based on Microphase Separation of Fullerene-Attached Thiophene-Selenophene Heteroblock Copolymers. ACS Applied Materials & Interfaces, 2017, 9, 4758-4768.	8.0	16
78	Crystallinity of the epitaxial heterojunction of C60 on single crystal pentacene. Journal of Crystal Growth, 2017, 468, 770-773.	1.5	14
79	Engineering Thin Films of a Tetrabenzoporphyrin toward Efficient Charge-Carrier Transport: Selective Formation of a Brickwork Motif. ACS Applied Materials & Interfaces, 2017, 9, 8211-8218.	8.0	16
80	Ï€-Conjugation Effects of Oligo(thienylenevinylene) Side Chains in Semiconducting Polymers on Photovoltaic Performance. Macromolecules, 2017, 50, 3557-3564.	4.8	6
81	The influence of branched alkyl side chains in A–D–A oligothiophenes on the photovoltaic performance and morphology of solution-processed bulk-heterojunction solar cells. Organic Chemistry Frontiers, 2017, 4, 1561-1573.	4.5	24
82	Time evolution studies of dithieno[3,2-b:2′,3′-d]pyrrole-based A–D–A oligothiophene bulk heterojunctions during solvent vapor annealing towards optimization of photocurrent generation. Journal of Materials Chemistry A, 2017, 5, 1005-1013.	10.3	19
83	Side-chain engineering in a thermal precursor approach for efficient photocurrent generation. Journal of Materials Chemistry A, 2017, 5, 14003-14011.	10.3	29
84	The effect of air exposure on the crystal structure of oligo-thiophene thin films investigated using in situ X-ray diffraction. Journal of Crystal Growth, 2017, 468, 816-820.	1.5	1
85	Regioisomer effects of [70]PCBM on film structures and photovoltaic properties of composite films with a crystalline conjugated polymer P3HT. RSC Advances, 2017, 7, 45697-45704.	3.6	10
86	Synthesis of regioblock copolythiophene by Negishi catalyst-transfer polycondensation using ^t Bu ₂ ZnA·2LiCl. Polymer Chemistry, 2017, 8, 6143-6149.	3.9	9
87	Magnetic Anisotropy and Damping for Monolayer-Controlled Co Ni Epitaxial Multilayer. Journal of the Physical Society of Japan, 2017, 86, 074710.	1.6	11
88	Formation of epitaxial Ti-Si-C Ohmic contact on 4H-SiC C face using pulsed-laser annealing. Applied Physics Letters, 2017, 110, .	3.3	17
89	Stable ultrathin surfactantâ€free surfaceâ€engineered silicon nanocrystal solar cells deposited at room temperature. Energy Science and Engineering, 2017, 5, 184-193.	4.0	11
90	Epitaxial Growth of C ₆₀ on Rubrene Single Crystals for a Highly Ordered Organic Donor/Acceptor Interface. Crystal Growth and Design, 2017, 17, 4622-4627.	3.0	17

#	Article	IF	CITATIONS
91	A Series of Lithium Pyridyl Phenolate Complexes with a Pendant Pyridyl Group for Electron-Injection Layers in Organic Light-Emitting Devices. ACS Applied Materials & Interfaces, 2017, 9, 40541-40548.	8.0	8
92	Uniaxial orientation of P3HT film prepared by soft friction transfer method. Scientific Reports, 2017, 7, 5141.	3.3	26
93	Regioisomer effects of [70]fullerene mono-adduct acceptors in bulk heterojunction polymer solar cells. Chemical Science, 2017, 8, 181-188.	7.4	52
94	Heteroepitaxy of Perfluoropentacene (C ₂₂ F ₁₄) on the Single Crystal Surface of Pentacene (C ₂₂ 14). Hyomen Kagaku, 2017, 38, 324-329.	0.0	4
95	Hard x-ray photoelectron spectroscopy equipment developed at beamline BL46XU of SPring-8 for industrial researches. AIP Conference Proceedings, 2016, , .	0.4	16
96	Square entimeter‧ized Highâ€Efficiency Polymer Solar Cells: How the Processing Atmosphere and Film Quality Influence Performance at Large Scale. Advanced Energy Materials, 2016, 6, 1600290.	19.5	26
97	Effects of applying bias voltage on metal-coated pentacene films on SiO2studied by hard X-ray photoelectron spectroscopy. Japanese Journal of Applied Physics, 2016, 55, 03DD09.	1.5	6
98	Relationship between photostability and nanostructures in DTS(FBTTh2)2:fullerene bulk-heterojunction films. Solar Energy Materials and Solar Cells, 2016, 151, 96-101.	6.2	7
99	Epitaxial Growth of an Organic p–n Heterojunction: C ₆₀ on Single-Crystal Pentacene. ACS Applied Materials & Interfaces, 2016, 8, 13499-13505.	8.0	49
100	Enhancement of Out-of-Plane Mobilities of Three Poly(3-alkylthiophene)s and Associated Mechanism. Journal of Physical Chemistry C, 2016, 120, 23351-23357.	3.1	23
101	Terazulene Isomers: Polarity Change of OFETs through Molecular Orbital Distribution Contrast. Journal of the American Chemical Society, 2016, 138, 11335-11343.	13.7	132
102	Performance of Si/PEDOT:PSS Hybrid Solar Cell Controlled by PEDOT:PSS Film Nanostructure. Journal of Physical Chemistry C, 2016, 120, 19043-19048.	3.1	46
103	Implication of Fluorine Atom on Electronic Properties, Ordering Structures, and Photovoltaic Performance in Naphthobisthiadiazole-Based Semiconducting Polymers. Journal of the American Chemical Society, 2016, 138, 10265-10275.	13.7	319
104	Thermal stabilization of organic photovoltaic cells using [6,6]-phenyl C61-butyric acid methyl ester analogs: Effects of alkyl substituents on the nanostructures of bulk heterojunction films and their stabilities. Synthetic Metals, 2016, 221, 61-66.	3.9	3
105	A new instrumentation for <i>in situ</i> characterization of the charge transport and crystallographic properties in co-evaporated organic thin film transistor. Molecular Crystals and Liquid Crystals, 2016, 636, 168-175.	0.9	4
106	Synthesis and FET characterization of novel ambipolar and lowâ€bandgap naphthaleneâ€diimideâ€based semiconducting polymers. Journal of Polymer Science Part A, 2016, 54, 359-367.	2.3	8
107	Photoprecursor Approach Enables Preparation of Well-Performing Bulk-Heterojunction Layers Comprising a Highly Aggregating Molecular Semiconductor. ACS Applied Materials & Interfaces, 2016, 8, 8644-8651.	8.0	11
108	Sequentially Different AB Diblock and ABA Triblock Copolymers as P3HT:PCBM Interfacial Compatibilizers for Bulk-Heterojunction Photovoltaics. ACS Applied Materials & Interfaces, 2016, 8, 5484-5492.	8.0	34

#	Article	IF	CITATIONS
109	Interface-induced crystallization and nanostructure formation of [6,6]-phenyl-C ₆₁ -butyric acid methyl ester (PCBM) in polymer blend films and its application in photovoltaics. Journal of Materials Chemistry A, 2016, 4, 3335-3341.	10.3	14
110	Amide-bridged terphenyl and dithienylbenzene units for semiconducting polymers. RSC Advances, 2016, 6, 16437-16447.	3.6	4
111	Structural Determination of the Epitaxial C ₆₀ Overlayer on the Pentacene Single Crystal by Grazing Incidence X-ray Diffraction. Hyomen Kagaku, 2016, 37, 429-434.	0.0	6
112	Hole mobility enhancement of MEH-PPV film by heat treatment at <i>T</i> g. AIP Advances, 2015, 5, .	1.3	13
113	Efficient inverted polymer solar cells employing favourable molecular orientation. Nature Photonics, 2015, 9, 403-408.	31.4	769
114	Oriented Thin Films of the Low-Band-Gap Polymer PTB7 by Friction Transfer Method. Molecular Crystals and Liquid Crystals, 2015, 621, 118-123.	0.9	3
115	Synthesis and Characterization of ABC-Type Asymmetric Star Polymers Comprised of Poly(3-hexylthiophene), Polystyrene, and Poly(2-vinylpyridine) Segments. Macromolecules, 2015, 48, 245-255.	4.8	33
116	Crystallization-Induced Energy Level Change of [6,6]-Phenyl-C ₆₁ -Butyric Acid Methyl Ester (PCBM) Film: Impact of Electronic Polarization Energy. Journal of Physical Chemistry C, 2015, 119, 23-28.	3.1	44
117	Synthesis, characterization, and application to polymer solar cells of polythiophene derivatives with ester- or ketone-substituted phenyl side groups. Journal of Polymer Science Part A, 2015, 53, 875-887.	2.3	6
118	Crystallization Dynamics of Organolead Halide Perovskite by Real-Time X-ray Diffraction. Nano Letters, 2015, 15, 5630-5634.	9.1	77
119	Synthesis and Isolation of <i>cis</i> -2 Regiospecific Ethylene-Tethered Indene Dimer–[70]Fullerene Adduct for Polymer Solar Cell Applications. ACS Applied Materials & Interfaces, 2015, 7, 16676-16685.	8.0	34
120	Thienothiopheneâ€2,5â€Dioneâ€Based Donor–Acceptor Polymers: Improved Synthesis and Influence of the Donor Units on Ambipolar Charge Transport Properties. Advanced Electronic Materials, 2015, 1, 1500039.	5.1	32
121	Synthesis of 1,3,4-thiadiazole-based donor–acceptor alternating copolymers for polymer solar cells with high open-circuit voltage. Polymer Journal, 2015, 47, 513-521.	2.7	12
122	Enhancement of Out-of-plane Mobility in P3HT Film by Rubbing: Aggregation and Planarity Enhanced with Low Regioregularity. Journal of Physical Chemistry C, 2015, 119, 7987-7995.	3.1	49
123	A single cis-2 regioisomer of ethylene-tethered indene dimer–fullerene adduct as an electron-acceptor in polymer solar cells. Chemical Communications, 2015, 51, 8233-8236.	4.1	36
124	Influence of 4â€fluorophenyl pendants in thieno[3,4â€b]thiopheneâ€benzo[1,2â€b:4,5â€bâ€2]dithiopheneâ€ba polymers on the performance of photovoltaics. Journal of Polymer Science Part A, 2015, 53, 1586-1593.	sed 2.3	3
125	Structural and magnetic properties of FeNi thin films fabricated on amorphous substrates. Journal of Applied Physics, 2015, 117, .	2.5	20
126	Molecular engineering of benzothienoisoindigo copolymers allowing highly preferential face-on orientations. Journal of Materials Chemistry A, 2015, 3, 21578-21585.	10.3	21

#	Article	IF	CITATIONS
127	Hard X-ray Photoemission Spectroscopy at Beamline BL46XU of SPring-8. Journal of Surface Analysis (Online), 2015, 21, 121-129.	0.1	13
128	â€Face-On―Oriented ^ ^pi;-Conjugated Polymers Containing 1,3,4-Thiadiazole Moiety Investigated with Synchrotron GIXS Measurements: Relationship between Morphology and PSC Performance. Journal of Photopolymer Science and Technology = [Fotoporima Konwakai Shi], 2014, 27, 351-356.	0.3	2
129	Microscopic structure and electrical transport property of sputter-deposited amorphous indium-gallium-zinc oxide semiconductor films. Journal of Physics: Conference Series, 2014, 518, 012001.	0.4	12
130	5, 10-linked naphthodithiophenes as the building block for semiconducting polymers. Science and Technology of Advanced Materials, 2014, 15, 024201.	6.1	5
131	Effect of Oxygen ontaining Functional Side Chains on the Electronic Properties and Photovoltaic Performances in a Thiophene–Thiazolothiazole Copolymer System. Heteroatom Chemistry, 2014, 25, 556-564.	0.7	6
132	Addition of Co to L1 ₀ -ordered FeNi films: influences on magnetic properties and ordered structures. Journal Physics D: Applied Physics, 2014, 47, 425001.	2.8	27
133	Crystal structure of oligothiophene thin films characterized by two-dimensional grazing incidence X-ray diffraction. Japanese Journal of Applied Physics, 2014, 53, 01AD01.	1.5	6
134	Novel dibenzo[a,e]pentalene-based conjugated polymers. Journal of Materials Chemistry C, 2014, 2, 64-70.	5.5	63
135	Thiophene–Thiazolothiazole Copolymers: Significant Impact of Side Chain Composition on Backbone Orientation and Solar Cell Performances. Advanced Materials, 2014, 26, 331-338.	21.0	275
136	Contrasting Effect of Alkylation on the Ordering Structure in Isomeric Naphthodithiophene-Based Polymers. Macromolecules, 2014, 47, 3502-3510.	4.8	36
137	Fe–Ni composition dependence of magnetic anisotropy in artificially fabricated L1 ₀ -ordered FeNi films. Journal of Physics Condensed Matter, 2014, 26, 064207.	1.8	82
138	Small band gap polymers incorporating a strong acceptor, thieno[3,2-b]thiophene-2,5-dione, with p-channel and ambipolar charge transport characteristics. Journal of Materials Chemistry C, 2014, 2, 2307-2312.	5.5	27
139	Enhanced vertical carrier mobility in poly(3-alkylthiophene) thin films sandwiched between self-assembled monolayers and surface-segregated layers. Chemical Communications, 2014, 50, 3627-3630.	4.1	27
140	Separated crystallization of donor and acceptor in oligo(p-phenylenevinylene)-naphthalenediimide dyad films. Synthetic Metals, 2014, 197, 175-181.	3.9	4
141	Effect of chemical ordering on 90° interlayer coupling in epitaxial Co–Fe/Cr/Co–Fe thin films. Journal of Magnetism and Magnetic Materials, 2014, 369, 211-218.	2.3	2
142	A HAXPES measurement system up to 15 keV developed at BL46XU of SPring-8. Journal of Physics: Conference Series, 2014, 502, 012006.	0.4	7
143	In-situ Observation of 2-Dimensional X-ray Diffraction of Organic Thin-film Growth by Synchrotron Radiation. Hyomen Kagaku, 2014, 35, 190-195.	0.0	1
144	Thickness of Crystalline Layer of Rubbed Polyimide Film Characterized by Grazing Incidence X-ray Diffractions with Multi Incident Angles. IEICE Transactions on Electronics, 2014, E97.C, 1089-1092.	0.6	3

#	Article	IF	CITATIONS
145	Fabrication of Fully-Epitaxial Co\$_{{{2}}\$MnSi/Ag/Co\$_{{{2}}\$MnSi Giant Magnetoresistive Devices by Elevated Temperature Deposition. IEEE Transactions on Magnetics, 2013, 49, 5464-5468.	2.1	6
146	Relation Between the Crystal Axis and the Strain Dependence of Critical Current Under Tensile Strain for GdBCO Coated Conductors. IEEE Transactions on Applied Superconductivity, 2013, 23, 8400304-8400304.	1.7	17
147	Microstructures of BPDA-PPD polyimide thin films with different thicknesses. Polymer, 2013, 54, 2435-2439.	3.8	17
148	End-On Orientation of Semiconducting Polymers in Thin Films Induced by Surface Segregation of Fluoroalkyl Chains. Journal of the American Chemical Society, 2013, 135, 9644-9647.	13.7	71
149	Naphthodithiophene–Naphthobisthiadiazole Copolymers for Solar Cells: Alkylation Drives the Polymer Backbone Flat and Promotes Efficiency. Journal of the American Chemical Society, 2013, 135, 8834-8837.	13.7	301
150	Control of residual strain and twin boundary by annealing under strain. Superconductor Science and Technology, 2013, 26, 065013.	3.5	5
151	Impact of Film Structure on Ionization Energy of Titanyl-Phthalocyanine in Thin Films. Materials Research Society Symposia Proceedings, 2013, 1605, 1.	0.1	0
152	Structure and magnetoresistance of current-perpendicular-to-plane pseudo spin valves using Co2Mn(Ga0.25Ge0.75) Heusler alloy. Journal of Applied Physics, 2013, 113, .	2.5	38
153	<i>In Situ</i> Real-Time X-Ray Diffraction During Thin Film Growth of Pentacene. Molecular Crystals and Liquid Crystals, 2012, 566, 18-21.	0.9	25
154	In situ Structural Study of Organic Semiconductor Thin Films. Materials Research Society Symposia Proceedings, 2012, 1402, 54.	0.1	1
155	Magnetic Anisotropy and Chemical Order of Artificially Synthesized L1 ₀ -Ordered FeNi Films on Au–Cu–Ni Buffer Layers. Japanese Journal of Applied Physics, 2012, 51, 010204.	1.5	37
156	Internal strain measurement for Nb ₃ Sn wires using synchrotron radiation. Superconductor Science and Technology, 2012, 25, 054004.	3.5	5
157	In situ structural characterization of picene thin films by X-ray scattering: Vacuum versus <mml:math xmlns:mml="http://www.w3.org/1998/Math/MathML" altimg="si10.gif" overflow="scroll"><mml:mrow><mml:msub><mml:mrow><mml:mtext>O</mml:mtext></mml:mrow><mml:mrov atmosphere. Chemical Physics Letters, 2012, 544, 34-38.</mml:mrov </mml:msub></mml:mrow></mml:math 	v> 2,6 mml:rr	ın≯2
158	Two Dimensional Grazing Incidence X-Ray Diffraction of TIPS-Pentacene Thin Films. Molecular Crystals and Liquid Crystals, 2012, 568, 134-138.	0.9	2
159	Naphthodithiophene-Based Donor–Acceptor Polymers: Versatile Semiconductors for OFETs and OPVs. ACS Macro Letters, 2012, 1, 437-440.	4.8	128
160	Strain Dependence of Superconducting Properties for GdBCO Coated Conductor in High Field Under Tensile Load. IEEE Transactions on Applied Superconductivity, 2012, 22, 6600504-6600504.	1.7	7
161	Quinacridone-Based Semiconducting Polymers: Implication of Electronic Structure and Orientational Order for Charge Transport Property. Chemistry of Materials, 2012, 24, 1235-1243.	6.7	68
162	Synthesis, Characterization, and Transistor and Solar Cell Applications of a Naphthobisthiadiazole-Based Semiconducting Polymer. Journal of the American Chemical Society, 2012, 134, 3498-3507.	13.7	323

#	Article	IF	CITATIONS
163	The effect of the 2D internal strain state on the critical current in GdBCO coated conductors. Superconductor Science and Technology, 2012, 25, 054014.	3.5	38
164	Drastic Change of Molecular Orientation in a Thiazolothiazole Copolymer by Molecularâ€Weight Control and Blending with PC ₆₁ BM Leads to High Efficiencies in Solar Cells. Advanced Materials, 2012, 24, 425-430.	21.0	157
165	Magnetic Anisotropy and Chemical Order of Artificially Synthesized L1 ₀ -Ordered FeNi Films on Au–Cu–Ni Buffer Layers. Japanese Journal of Applied Physics, 2012, 51, 010204.	1.5	13
166	Orientation of Crystalline and Non-crystalline PMDA-ODA Polymers at Rubbed Film Surface. IEICE Transactions on Electronics, 2012, E95.C, 1749-1751.	0.6	0
167	Bending strain analysis considering a shift of the neutral axis for YBCO coated conductors with and without a Cu stabilizing layer. Superconductor Science and Technology, 2011, 24, 075019.	3.5	28
168	Artificial Fabrication and Order Parameter Estimation of L10-ordered FeNi Thin Film Grown on a AuNi Buffer Layer. Journal of the Magnetics Society of Japan, 2011, 35, 370-373.	0.9	60
169	Molecular Aggregation States of Imogolite/P3HT Nanofiber Hybrid. Journal of Physics: Conference Series, 2011, 272, 012021.	0.4	7
170	Development of a CdTe pixel detector with a window comparator ASIC for high energy X-ray applications. Nuclear Instruments and Methods in Physics Research, Section A: Accelerators, Spectrometers, Detectors and Associated Equipment, 2011, 650, 88-91.	1.6	13
171	Evaluation of Properties of SiO ₂ Films Fabricated by Plasma Oxidation. ECS Transactions, 2011, 41, 169-175.	0.5	3
172	Characterization of Vertical Alignment Film by X-Ray Reflectivity. IEICE Transactions on Electronics, 2011, E94-C, 1755-1759.	0.6	1
173	Improvement in Stability of SPring-8 Standard X-Ray Monochromators with Water-Cooled Crystals. AIP Conference Proceedings, 2010, , .	0.4	3
174	Suppression Mechanism of Volume Shrinkage for SOG Film by Plasma Treatment. ECS Transactions, 2010, 28, 347-354.	0.5	1
175	Study of Charge Trap Sites in SiN Films by Hard X-ray Photoelectron Spectroscopy. Japanese Journal of Applied Physics, 2010, 49, 04DD11.	1.5	4
176	Evaluation and Control of Strain in Si Induced by Patterned SiN Stressor. Electrochemical and Solid-State Letters, 2009, 12, H117.	2.2	10
177	Design optimization of highly accurate elliptical mirrors for hard-x-ray microfocusing probes at SPring-8. , 2009, , .		14
178	Improvement of CVD SiO2 by Post Deposition Microwave Plasma Treatment. ECS Transactions, 2009, 19, 45-51.	0.5	9
179	Characterization of Liquid Crystal Alignment on Rubbed Polyimide Film by Grazing-Incidence X-Ray Diffraction. IEICE Transactions on Electronics, 2009, E92-C, 1371-1375.	0.6	1
180	Effects of Annealing on Rubbed Polyimide Surface Studiedby Grazing-Incidence X-Ray Diffraction. IEICE Transactions on Electronics, 2009, E92-C, 1376-1381.	0.6	7

#	Article	IF	CITATIONS
181	Development of a high-precision slit for x-ray beamline at SPring-8. Proceedings of SPIE, 2009, , .	0.8	0
182	Crystallographic coherent lengths of J-aggregates and their absorption spectra. Colloids and Surfaces A: Physicochemical and Engineering Aspects, 2008, 321, 275-280.	4.7	2
183	A hydrogen storage layer on the surface of silicon nitride films. Applied Physics Letters, 2008, 92, .	3.3	17
184	Evaluation and Control of Strain in Si Induced by Patterned SiN Stressor. ECS Transactions, 2008, 13, 263-269.	0.5	0
185	Dependence of Kind of Solvents for Washing on Surface of Rubbed Polyimide Film. IEICE Transactions on Electronics, 2008, E91-C, 1587-1592.	0.6	0
186	Effects of Rubbing Condition and Soaking Time on Surface Crystallization of Rubbed Polyimide Film by Soaking into Acetone. IEICE Transactions on Electronics, 2008, E91-C, 1593-1598.	0.6	1
187	ANISOTROPY OF MULTILAYERED (CU , C) BA ₂ CA ₃ CUSUPERCONDUCTORS STUDIED BY TORQUE MAGNETOMETRY. International Journal of Modern Physics B, 2007, 21, 3285-3289.	ont> _{ 2.0}	4 <for< td=""></for<>
188	Reinterpretation of the unit cell evolution of BaTiO3. Physics Letters, Section A: General, Atomic and Solid State Physics, 2007, 367, 394-401.	2.1	13
189	Effect of Rubbing on Polymers for Liquid Crystal Alignment Film Studied by Grazing-Incidence X-ray Diffraction and Reflection Ellipsometry. IEICE Transactions on Electronics, 2007, E90-C, 2070-2075.	0.6	5
190	New finding of coherent hybrid structure of BaTiO3 single crystal in the room temperature phase. Physics Letters, Section A: General, Atomic and Solid State Physics, 2006, 353, 250-254.	2.1	16
191	A Diffraction System with an X-ray Beam of a Band of Wavelengths. AIP Conference Proceedings, 2004, , \cdot	0.4	0
192	A wide-bandpass multilayer monochromator and its application to the determination of absolute structure. Journal of Applied Crystallography, 2004, 37, 136-142.	4.5	0
193	The effect of pinning centers in Zn-doped CuBa2Ca3Cu4O12â^'y high-temperature superconductors. Journal of Physics and Chemistry of Solids, 2002, 63, 1073-1076.	4.0	12
194	Wavelength-Modulated Diffraction System. Nuclear Instruments and Methods in Physics Research, Section A: Accelerators, Spectrometers, Detectors and Associated Equipment, 2001, 467-468, 1053-1056.	1.6	0
195	Phase determination by wavelength-modulated diffraction. I. Centrosymmetric case. Journal of Synchrotron Radiation, 2001, 8, 1035-1039.	2.4	1
196	Optimization of Ni/Nb Ratio for High-Temperature-Reliable Ni/Nb Silicide Ohmic Contact on 4H-SiC. Materials Science Forum, 0, 963, 498-501.	0.3	0